MUC1 Oncoprotein Functions in Activation of Fibroblast Growth Factor Receptor Signaling

Jian Ren, Deepak Raina, Wen Chen, Guilan Li, Lei Huang, and Donald Kufe

Dana-Farber Cancer Institute, Harvard Medical School, Boston, Massachusetts

Abstract

Activation of the fibroblast growth factor (FGF) receptor 3 (FGFR3) has been linked to the development of human cancers by mechanisms that are not well understood. The MUC1 oncoprotein is aberrantly overexpressed by certain hematologic malignancies and most human carcinomas. The present studies show that MUC1 associates with FGFR3. Stimulation of cells with FGF1 increased the interaction between MUC1 and FGFR3. FGF1 stimulation also induced c-Src-dependent tyrosine phosphorylation of the MUC1 cytoplasmic domain on a YEKV motif. FGF1-induced tyrosine phosphorylation of MUC1 was associated with increased binding of MUC1 to β-catenin and targeting of MUC1 and β-catenin to the nucleus. FGF1 also induced binding of MUC1 to the heat shock protein 90 (HSP90) chaperone by a mechanism dependent on phosphorylation of the YEKV motif. Notably, β-catenin and HSP90 compete for binding to the MUC1 cytoplasmic domain, indicating that MUC1 forms mutually exclusive complexes with these proteins. The results also show that inhibition of HSP90 with geldanamycin or 17-(allylamino)-17-demethoxygeldanamycin attenuates FGF1-induced binding of MUC1 to HSP90 and targeting of MUC1 to the mitochondrial outer membrane. These findings indicate that FGF1 induces phosphorylation of MUC1 on YEKV and thereby activates two distinct pathways: (*a*) nuclear localization of MUC1 and β-catenin and (*b*) delivery of MUC1 to mitochondria by HSP90. (Mol Cancer Res 2006;4(11):873–83)

Introduction

The MUC1 integral membrane protein is expressed at the apical borders of normal secretory epithelial cells and aberrantly at high levels over the entire surface of carcinoma cells (1). MUC1 is translated as a single polypeptide and undergoes autocleavage into two subunits that form a heterodimeric complex (2-4). The MUC1 NH_2-terminal ectodomain (MUC1 N-ter, MUC1-N) consists of variable numbers of 20 amino acid tandem repeats, which are modified by O-linked glycans (5, 6). The MUC1 COOH-terminal subunit (MUC1 C-ter, MUC1-C) includes a 58-amino acid extracellular domain, a transmembrane domain, and a 72-amino acid cytoplasmic tail (7). The >250-kDa MUC1-N ectodomain associates with the ~25-kDa MUC1-C as a heterodimer or, in response to certain stimuli, is released from the cell surface (2). Importantly, overexpression of MUC1 confers transformation and blocks the apoptotic response to anticancer agents (8-12). MUC1 interacts with members of the ErbB family of receptor tyrosine kinases (13-15). Stimulation of cells with the epidermal growth factor (EGF) induces tyrosine phosphorylation of the MUC1 cytoplasmic domain (MUC1-CD) and binding of MUC1 to the Wnt effector β-catenin (13, 16-18). Moreover, heregulin stimulates interactions between MUC1 and ErbB2, ErbB3, and ErbB4 and binding of MUC1-C to β-catenin and the related γ-catenin (15). Heregulin also targets MUC1-C, but not MUC1-N, to mitochondria (10). These findings have indicated that MUC1-C functions in transducing signals from activated ErbB receptors to the interior of the cell. MUC1 is not known to interact with other cell surface receptors.

The fibroblast growth factor (FGF) receptor (FGFR) family of receptor tyrosine kinases consists of four related members that have been designated FGFR1, FGFR2, FGFR3, and FGFR4. The FGFRs contain three extracellular immunoglobulin (Ig) domains, a transmembrane region, and an intracellular cytoplasmic tail with a divided tyrosine kinase domain (19). Activation of FGFRs by the FGF family of ligands results in receptor dimerization and transphosphorylation of the intracellular domains on tyrosine (19). Mutations in the genes encoding the FGFRs confer several different disorders that affect skeletal development (20). Mutations and translocations of the FGFRs have also been associated with human cancers (21-25). In particular, mutations that result in aberrant activation of FGFR3 have been found in bladder carcinomas, cervical carcinomas, and multiple myeloma (26-28). The t(4;14) translocation that results in FGFR3 activation in multiple myeloma cells is associated with increased proliferation (27-31). Moreover, silencing FGFR3 induces apoptosis of multiple myeloma cells (32). Overexpression of FGFR3 has also been linked to the development of bladder cancer (33). FGFR3 has been shown to signal activation of signal transducers and activators of transcription 1, 3, and 5 (34-37). Otherwise, little is known about how FGFR3 may contribute to transformation (38).

The present results show that MUC1 associates with FGFR3 and that this interaction is increased by FGF1. We show that FGF1 induces phosphorylation of MUC1-C on a YEKV motif in the cytoplasmic tail and thereby binding of

Received 7/10/06; revised 9/5/06; accepted 9/13/06.
Grant support: National Cancer Institute grants CA100707 and CA97098.
The costs of publication of this article were defrayed in part by the payment of page charges. This article must therefore be hereby marked advertisement in accordance with 18 U.S.C. Section 1734 solely to indicate this fact.
Requests for reprints: Donald Kufe, Dana-Farber Cancer Institute, 44 Binney Street, Boston, MA 02115. Phone: 617-632-3141; Fax: 617-632-2934. E-mail: donald_kufe@dfci.harvard.edu

doi:10.1158/1541-7786.MCR-06-0204

MUC1 to β-catenin or the heat shock protein (HSP) 90 chaperone. The results also show that FGF1 induces targeting of MUC1-C to the nucleus with β-catenin and to mitochondria by a HSP90-dependent mechanism.

Results

MUC1 Associates with FGFR3

To determine if FGFR3 forms a complex with MUC1, anti-FGFR3 immunoprecipitates from human ZR-75-1 breast cancer cell lysates were analyzed by immunoblotting with anti-MUC1. The results show that MUC1 coprecipitates with FGFR3 (Fig. 1A, *left*). Analysis of the immunoprecipitates with anti-FGFR3 confirmed precipitation of FGFR3 (Fig. 1A, *left*). As a control, there was no detectable MUC1 or FGFR3 in precipitates prepared with nonimmune rabbit IgG (Fig. 1A, *left*). In the reciprocal experiment, analysis of anti-MUC1 immunoprecipitates with anti-FGFR3 confirmed that MUC1 associates with FGFR3 (Fig. 1A, *right*). To assess whether activation of FGFR3 affects the interaction with MUC1, ZR-75-1 cells were stimulated with FGF1. Immunoblot analysis of anti-MUC1 immunoprecipitates with anti-FGFR3 showed that FGF1 increases the association between FGFR3 and MUC1 (Fig. 1B). To confirm this interaction, HCT116 colon cancer cells, which are null for endogenous MUC1 expression, were stably transfected to express an empty vector, MUC1, or

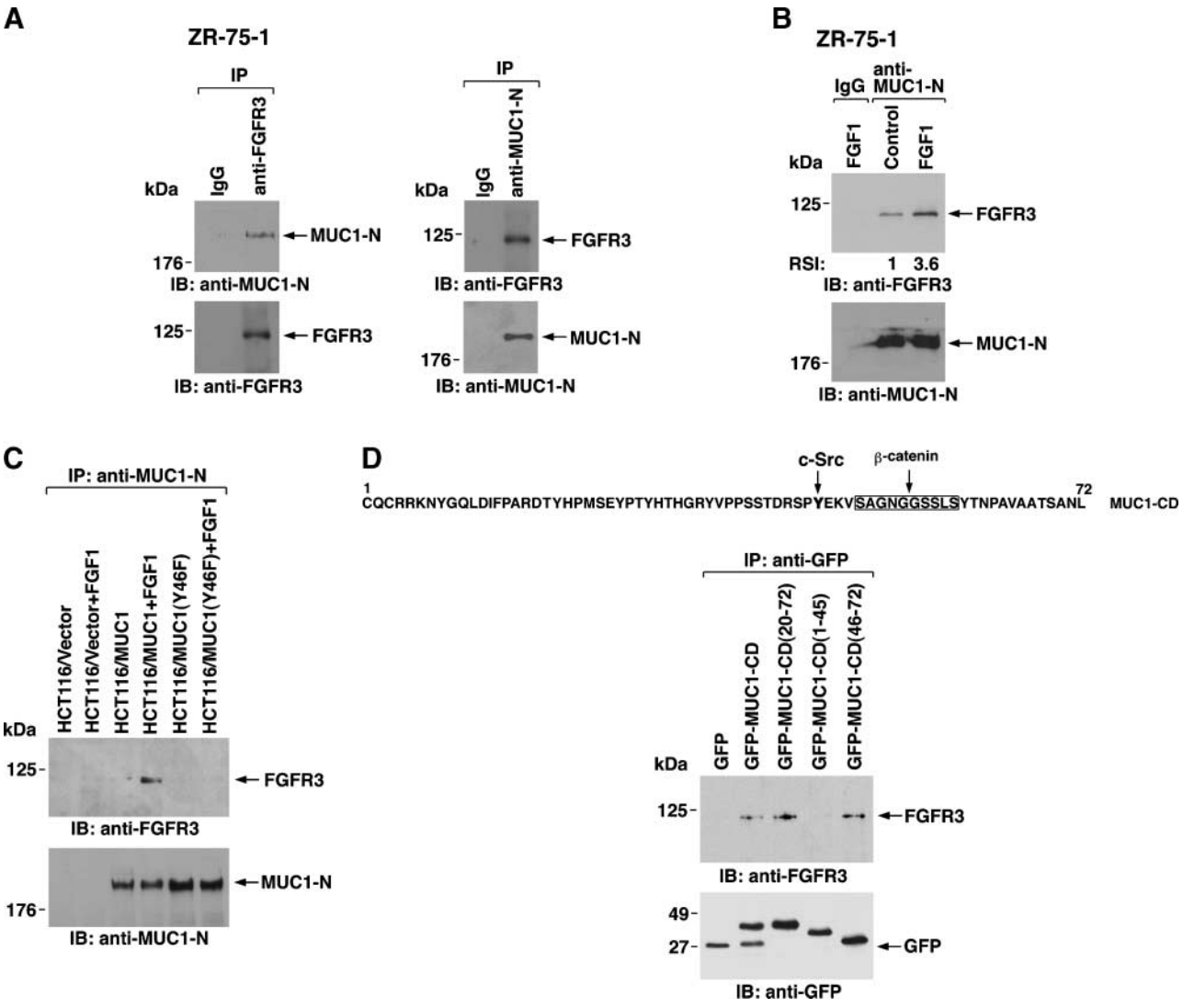

FIGURE 1. MUC1 associates with FGFR3. **A.** Lysates from ZR-75-1 cells were immunoprecipitated (*IP*) with anti-FGFR3 (*left*) or anti-MUC1-N (*right*). Nonimmune IgG was used as a control. The precipitates were immunoblotted (*IB*) with the indicated antibodies. **B.** ZR-75-1 cells were incubated in the absence of FGF1 (*Control*) or stimulated with 30 ng/mL FGF1 for 5 minutes. Anti-MUC1-N or nonimmune IgG precipitates were immunoblotted with anti-FGFR3 and anti-MUC1-N. The intensities of the signals were determined by densitometric scanning and are expressed as the relative signal intensity (*RSI*) compared with that obtained with the control. **C.** HCT116/vector, HCT116/MUC1, and HCT116/MUC1(Y46F) cells were stimulated with 30 ng/mL FGF1 for 5 minutes. Anti-MUC1-N precipitates were immunoblotted with the indicated antibodies. **D.** Top, amino acid sequence of MUC1-CD. The c-Src phosphorylation site and the β-catenin binding motif are highlighted. Bottom, 293 cells were transiently transfected with GFP or the indicated GFP-MUC1-CD fusion proteins and harvested at 48 hours. Anti-GFP precipitates were immunoblotted with anti-FGFR3 and anti-GFP. The lower band in lane 2 is GFP.

MUC1(Y46F) mutant. Tyr^{46} is the residue within the YEKV motif in the MUC1-CD that is phosphorylated by c-Src (18). FGF1 stimulation was associated with binding of FGFR3 and MUC1 in HCT116/MUC1, but not in HCT116/vector or HCT116/MUC1(Y46F), cells (Fig. 1C), suggesting that the MUC1-CD is functional in this interaction. Consequently, we overexpressed green fluorescent protein (GFP)-tagged MUC1-CD or MUC1-CD fragments in 293 cells. Immunoblot analysis of anti-GFP immunoprecipitates with anti-FGFR3 showed that MUC1-CD associates with FGFR3 (Fig. 1D). MUC1-CD(20-72) and MUC1-CD(46-72), but not MUC1-CD(1-45), also formed complexes with FGFR3 (Fig. 1D), indicating that MUC1-CD amino acids 46 to 72 are sufficient for the interaction. These findings indicate that (*a*) MUC1 associates with FGFR3, (*b*) activation of FGFR3 increases the association with MUC1, and (*c*) MUC1-CD is of importance in forming complexes with FGFR3.

FGF1 Induces Binding of MUC1 and β-Catenin

EGF stimulation is associated with phosphorylation of MUC1 on Tyr^{46} (13). To determine if FGF1 induces a similar response, lysates from ZR-75-1 breast cancer cells stably transfected to express a MUC1 small interfering RNA (siRNA) or, as a control, the empty vector (10) were analyzed by immunoblotting with an antibody against phosphorylated MUC1-Tyr^{46} (Fig. 2A). A low level of MUC1-Tyr^{46} phosphorylation was detectable in control ZR-75-1/vector cell lysates (Fig. 2A). By contrast, there was no detectable anti-phosphorylated MUC1-Tyr^{46} reactivity in cells silenced for MUC1 (Fig. 2A). Stimulation with FGF1 for 10 minutes was associated with a substantial increase in anti-phosphorylated MUC1-Tyr^{46} reactivity (Fig. 2B, *left*). Quantitation of the intensity of the signals by densitometric scanning showed over a 2-fold increase at 10 to 30 minutes of FGF1 stimulation in three separate experiments (Fig. 2B, *right*). Moreover, stimulation with FGF1 for 1 hour was associated with a return toward baseline levels of MUC1-Tyr^{46} phosphorylation (Fig. 2B, *right*). Previous work showed that MUC1-Tyr^{46} is phosphorylated by c-Src in heregulin-stimulated cells (39). In the present studies, treatment of the ZR-75-1 cells with 4-amino-5-(4-chlorophenyl)-7-(t-butyl)pyrazolo(3,4-d)pyrimidine (PP2), an inhibitor of c-Src, blocked FGF1-induced phosphorylation of MUC1 on Tyr^{46}, indicating that this response is mediated by a c-Src-dependent mechanism (Fig. 2B). As a control, there was no detectable effect of FGF1 stimulation on MUC1-C levels (Fig. 2B, *left*). We previously reported that EGF stimulation of HCT116/MUC1 cells induces phosphorylation of MUC1 on Tyr^{46} (18). Similar results were obtained when lysates from EGF-stimulated ZR-75-1 cells were immunoblotted with anti-phosphorylated MUC1-Tyr^{46} (Fig. 2C, *left*). Quantitation of the intensity of signals obtained in three experiments showed that EGF induces similar levels of MUC1-Tyr^{46} phosphorylation as found in the FGF1-stimulated cells (Fig. 2C, *right*). Moreover, like FGF1, the response to EGF was sensitive to PP2 treatment (Fig. 2C). Phosphorylation of MUC1 on Tyr^{46} increases the interaction between MUC1 and β-catenin (13, 18). Consistent with those findings and FGF1-induced phosphorylation of Tyr^{46}, FGF1 stimulation of ZR-75-1 cells was associated with increases in MUC1-β-catenin complexes (Fig. 2D). In HCT116 cells, FGF1 also induced binding of MUC1 and β-catenin (Fig. 2E). Moreover, this response was abrogated in HCT116 cells expressing MUC1 with a Y46F mutation (Fig. 2E). These findings indicate that FGF1 stimulation is associated with increased (*a*) phosphorylation of MUC1 on Tyr^{46} and (*b*) binding of MUC1 and β-catenin.

FGF1 Targets MUC1 to the Cytosol and Nucleus

MUC1 accumulates in the cytosol of transformed cells (1, 39-42). In concert with these findings, MUC1-C was detectable in the cytosol of ZR-75-1 cells (Fig. 3A). Moreover, stimulation of ZR-75-1 cells with FGF1 was associated with an increase in cytosolic MUC1-C levels (Fig. 3A, *left*). Quantitation of the signals from three experiments showed an ~2-fold increase in MUC1-C in the cytosol (Fig. 3A, *right*). Purity of the cytosolic preparations was confirmed by immunoblotting with antibodies against the cell membrane–associated platelet-derived growth factor receptor, endoplasmic reticulum–associated BAP31 (43), and the mitochondria-associated Tom20 proteins (Fig. 3A). A similar increase in cytosolic MUC1-C levels was observed when HCT116/MUC1 cells were stimulated with FGF1 (Fig. 3B), indicating that this response is not cell type specific. Other studies have shown that MUC1-C, but not MUC1-N, is trafficked to the nucleus (8, 9, 11, 44, 45). Analysis of purified nuclei from ZR-75-1 cells showed that FGF1 increases MUC1-C levels (Fig. 3C). Consistent with recent findings that β-catenin is stabilized by direct binding to MUC1 and that MUC1 targets β-catenin to the nucleus (46), nuclear levels of β-catenin were also increased over 2-fold in the response to FGF1 stimulation (Fig. 3C). Targeting of MUC1-C to the nucleus by FGF1 was confirmed in HCT116/MUC1 cells (Fig. 3D). However, in concert with previous results (46), the FGF1-induced interaction between MUC1 and β-catenin had no effect on nuclear β-catenin levels in HCT116 cells (Fig. 3D), which express a mutant β-catenin with deletion of Ser^{45}. This mutation abrogates the glycogen synthase kinase 3β phosphorylation-dependent binding of β-catenin with β-TrCP and thereby confers deregulated stability of β-catenin (47-50). These findings indicate that FGF1 regulates targeting of MUC1 to the cytosol and nucleus.

FGF1 Induces Binding of MUC1-C to HSP90

Recent studies showed that heregulin targets MUC1-C to mitochondria (10) and that this response is mediated by the HSP70 and HSP90 chaperones (39). As found with heregulin (39), FGF1 stimulation had little if any effect on binding of MUC1-C to HSP70 in HCT116/MUC1 (Fig. 4A) and ZR-75-1 (data not shown) cells. Stimulation of HCT116/MUC1 cells with FGF1 was, however, associated with increased binding of MUC1-C to HSP90, and this response was similar to that observed with heregulin (Fig. 4B). FGF1 also induced binding of MUC1-C to HSP90 in ZR-75-1 cells (Fig. 4C). In heregulin-stimulated cells, binding of MUC1-C to HSP90 is mediated by phosphorylation of MUC1 on Tyr^{46} (39). FGF1-induced interaction between MUC1-C and HSP90 was attenuated by expression of MUC1 with the Y46F mutation (Fig. 4D). These findings indicate that binding of MUC1-C to HSP90 is induced in the response of cells to FGF1 stimulation.

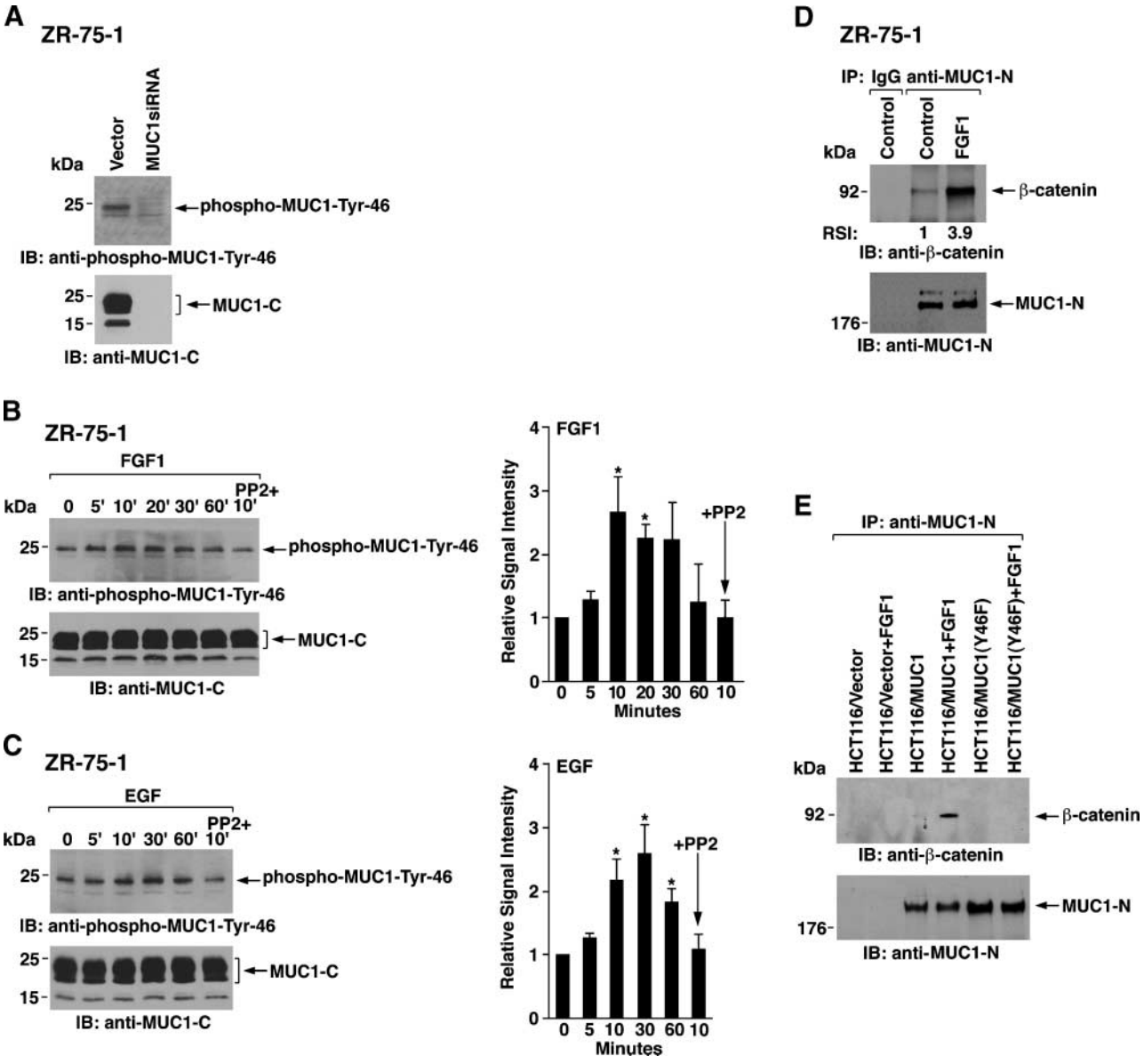

FIGURE 2. FGF1 induces MUC1 phosphorylation and binding of MUC1 to β-catenin. **A.** Lysates from ZR-75-1/vector and ZR-75-1/MUC1siRNA cells were immunoblotted with anti-phosphorylated MUC1-Tyr[46] (*phospho-MUC1-Tyr-46*) and anti-MUC1-C. **B** and **C.** ZR-75-1 cells were stimulated with FGF1 (**B**) or EGF (**C**) in the presence or absence of PP2 for the indicated times. Left, lysates were immunoblotted with the indicated antibodies. The intensities of the signals were determined by densitometric scanning. Right, results are expressed as the RSI compared with that obtained with the control (assigned a value of 1). Columns, mean of three separate experiments; bars, SE. *, $P < 0.05$, compared with control. **D.** ZR-75-1 cells were stimulated with FGF1 for 5 minutes. Anti-MUC1-N or control IgG precipitates were immunoblotted with anti-β-catenin and anti-MUC1-N. The RSI is compared with that of the control (designated as 1). **E.** HCT116/vector, HCT116/MUC1, and HCT116/MUC1(Y46F) cells were stimulated with FGF1 for 5 minutes. Anti-MUC1-N precipitates were immunoblotted with the indicated antibodies.

β-Catenin Competes with HSP70/HSP90 for Binding to the MUC1-CD

The results thus indicate that FGF1-induced phosphorylation of MUC1 on Tyr[46] increases binding of β-catenin and HSP90. We therefore asked whether binding of MUC1 to β-catenin and HSP90 is a mutually exclusive event. Previous work has shown that (*a*) β-catenin binds to a serine-rich motif (SRM) in the COOH-terminal region of the MUC1-CD, (*b*) this binding is increased by c-Src phosphorylation of MUC1-CD, and (*c*) mutation of the SRM abrogates the interaction (13, 16-18, 46). Other studies have shown that HSP70 binds to the MUC1-CD COOH-terminal region (39). The present results show that, in contrast to β-catenin, direct binding of MUC1-CD to HSP70 is not abrogated by mutation of the SRM (Fig. 5A). As shown previously (39), direct binding to HSP90 was dependent on c-Src phosphorylation of MUC1-CD (Fig. 5B). Moreover, there was no detectable HSP90 binding to c-Src-phosphorylated MUC1-CD with a mutated SRM (Fig. 5B), indicating that β-catenin and HSP90 may both interact with this region. In competition experiments, incubation of MUC1-CD with HSP70

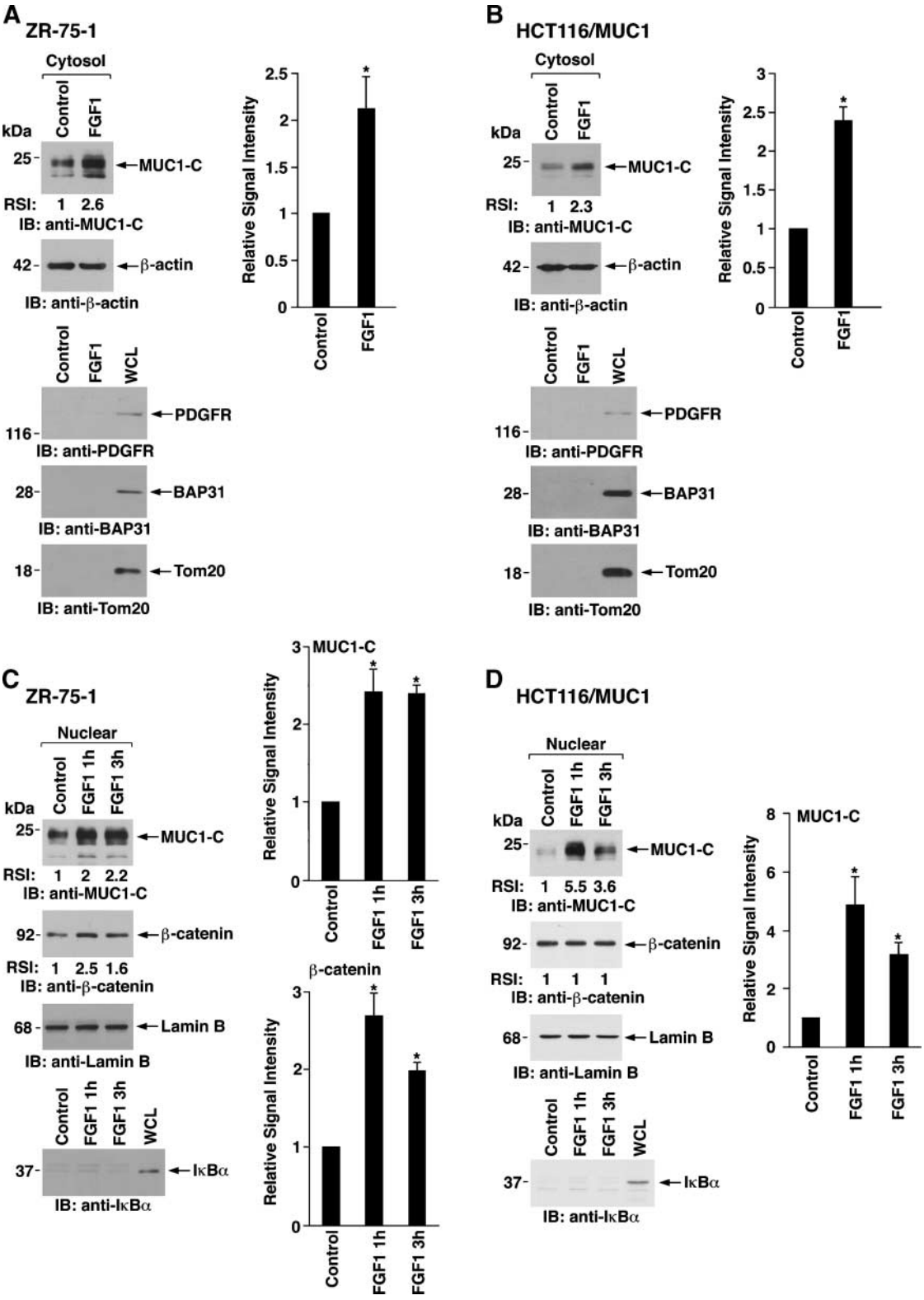

FIGURE 3. FGF1 targets MUC1 to the cytosol and nucleus. **A** and **B.** ZR-75-1 (**A**) and HCT116/MUC1 (**B**) cells were stimulated with FGF1 for 10 minutes. Left, cytosolic fractions were immunoblotted with the indicated antibodies. Whole-cell lysate (*WCL*) was included as a control. Right, results are expressed as the RSI compared with that obtained with the control (assigned a value of 1). Columns, mean of three separate experiments; bars, SE. *, $P < 0.05$, compared with control. **C** and **D.** ZR-75-1 (**C**) and HCT116/MUC1 (**D**) cells were stimulated with FGF1 for 1 and 3 hours. Left, nuclear fractions were immunoblotted with the indicated antibodies. Whole-cell lysate was used as a control. Right, results are expressed as the RSI compared with that obtained with the control (assigned a value of 1). Columns, mean of three separate experiments; bars, SE. *, $P < 0.05$, compared with control.

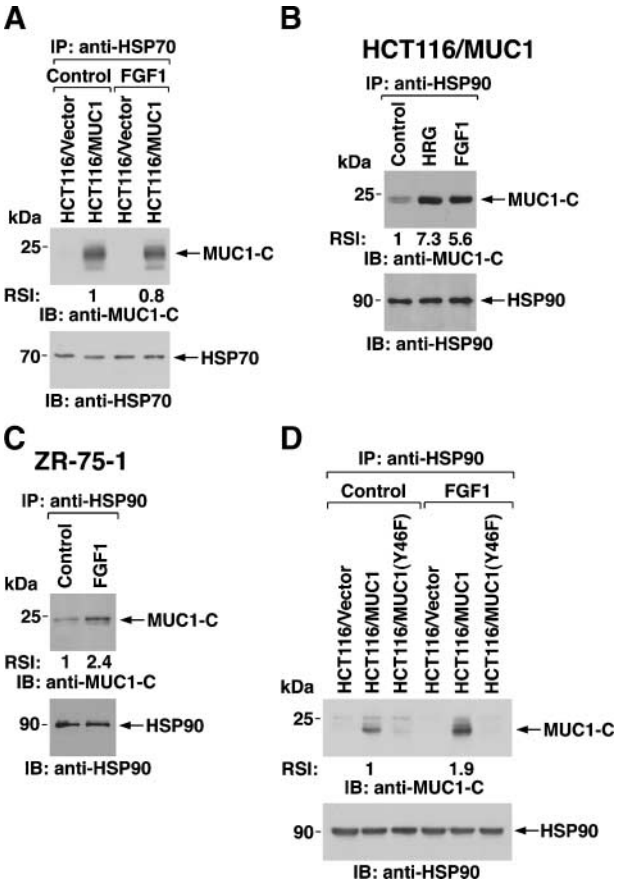

FIGURE 4. FGF1 induces binding of MUC1 and HSP90. **A.** HCT116/vector and HCT116/MUC1 cells were stimulated with FGF1 for 10 minutes. Anti-HSP70 precipitates were immunoblotted with anti-MUC1-C and anti-HSP70. **B.** HCT116/MUC1 cells were stimulated with heregulin (*HRG*) or FGF1 for 10 minutes. Anti-HSP90 precipitates were immunoblotted with anti-MUC1-C and anti-HSP90. **C.** ZR-75-1 cells were stimulated with FGF1 for 10 minutes. Anti-HSP90 precipitates were immunoblotted with the indicated antibodies. **D.** HCT116/vector, HCT116/MUC1, and HCT116/MUC1(Y46F) cells were stimulated with FGF1 for 10 minutes. Anti-HSP90 precipitates were immunoblotted with anti-MUC1-C and anti-HSP90. The RSI is compared with that obtained for the control (assigned a value of 1).

and then increasing amounts of β-catenin was associated with a progressive decrease in the interaction between MUC1-CD and HSP70 (Fig. 5C). In addition, β-catenin was more effective in competing with HSP90 for binding to MUC1-CD that had been phosphorylated by c-Src (Fig. 5D). These findings indicate that MUC1 forms mutually exclusive complexes with β-catenin and HSP70/HSP90.

FGF1 Targets MUC1-C to Mitochondria by a HSP90-Dependent Mechanism

To further assess FGF1-induced binding of MUC1-C to HSP90, we treated cells with geldanamycin, an inhibitor of HSP90 function (51). Geldanamycin had no effect on the interaction between MUC1 and HSP70 (Fig. 6A) but blocked the FGF1-induced binding of MUC1 and HSP90 (Fig. 6B). The HSP70/HSP90 complex functions in the delivery of client proteins to the mitochondrial outer membrane (52). In this regard, FGF1 stimulation was associated with increased targeting of MUC1 to mitochondria (Fig. 6C). Immunoblot analysis with antibodies against the nuclear proliferating cell nuclear antigen and cytosolic IκBα proteins further indicated that the mitochondria were not significantly contaminated with these fractions (Fig. 6C). In addition and consistent with involvement of HSP90, treatment with geldanamycin blocked FGF1-induced targeting of MUC1 to mitochondria (Fig. 6C). To confirm these results, we treated cells with 17-(allylamino)-17-demethoxygeldanamycin (17-AAG), another inhibitor of HSP90 (53). As found with geldanamycin, FGF1-induced increases in mitochondrial MUC1-C were blocked by 17-AAG (Fig. 6D). These findings indicate that FGF1 targets MUC1 to mitochondria by a HSP90-dependent mechanism.

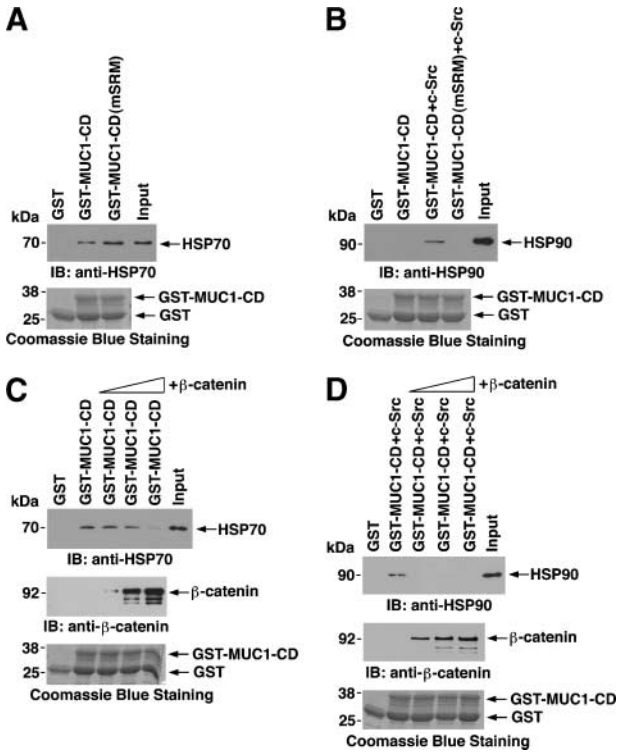

FIGURE 5. MUC1-C forms mutually exclusive complexes with β-catenin and HSP70/HSP90. **A.** GST, GST-MUC1-CD, and GST-MUC1-CD(mSRM) bound to glutathione beads were incubated with recombinant HSP70. The adsorbates were immunoblotted with anti-HSP70. Input lane, amount of HSP70 added to the reactions. Loading of the GST proteins was assessed by Coomassie blue staining. **B.** The indicated GST proteins bound to glutathione beads were incubated in the presence and absence of c-Src and ATP for 30 minutes at 30°C. Recombinant HSP90 was then added for 1 hour at 4°C. The adsorbates were analyzed by immunoblotting with anti-HSP90. **C.** GST-MUC1-CD bound to glutathione beads was incubated with HSP70 and then increasing amounts of β-catenin. The adsorbates were immunoblotted with anti-HSP70. Input of β-catenin was assessed by immunoblotting with anti-β-catenin. The molar ratio of HSP70 to β-catenin in the reactions was 1:2 (*lane 3*), 1:4 (*lane 4*), and 1:6 (*lane 5*). Input of the GST proteins was assessed by Coomassie blue staining. **D.** GST-MUC1-CD bound to glutathione beads was phosphorylated with c-Src and incubated with HSP90 as described in **B**. Increasing amounts of β-catenin were added to the reaction. The adsorbates were immunoblotted with anti-HSP90. Input of β-catenin was assessed by immunoblotting with anti-β-catenin. The molar ratio of HSP90 to β-catenin in the reactions was 5:1 (*lane 3*), 5:2 (*lane 4*), and 5:3 (*lane 5*). Input of the GST proteins was assessed by Coomassie blue staining.

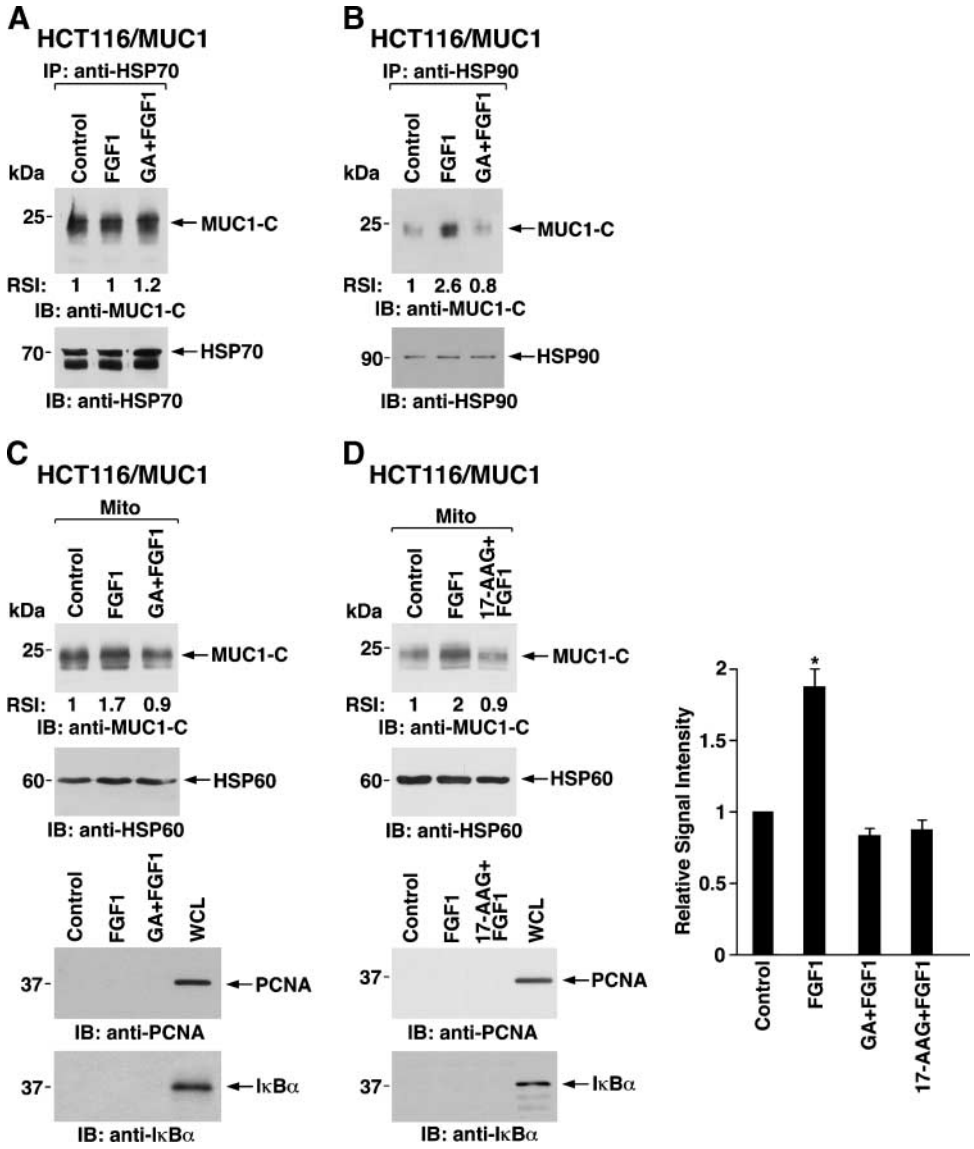

FIGURE 6. FGF1 targets MUC1 to mitochondria by a HSP90-dependent mechanism. **A** and **B.** HCT116/MUC1 cells were treated with FGF1 for 1 hour (*lane 2*) or 1 μmol/L geldanamycin (*GA*) for 1 hour and then FGF1 for 1 hour (*lane 3*). Anti-HSP70 (**A**) and anti-HSP90 (**B**) precipitates were immunoblotted with the indicated antibodies. **C** and **D.** HCT116/MUC1 cells were treated with FGF1 for 1 hour (*lane 2*), 1 μmol/L geldanamycin for 1 hour, and then FGF1 for 1 hour (**C**, *lane 3*) or 1 μmol/L 17-AAG for 1 hour and then FGF1 for 1 hour (**D**, *lane 3*). Left, purified mitochondria were immunoblotted with the indicated antibodies. Whole-cell lysate was included as a control. Right, results are expressed as the RSI compared with that obtained with the control (assigned a value of 1). Columns, mean of three separate experiments; bars, SE. *, $P < 0.05$, compared with control.

Discussion

MUC1 Interacts with FGFR3

MUC1 is expressed at the cell membrane as a heterodimer of the MUC1-N and MUC1-C subunits. Under physiologic conditions, MUC1 localizes to the apical borders of normal secretory epithelia (1). However, with transformation and loss of polarity, MUC1 is overexpressed throughout the entire cell membrane of carcinoma cells (1), allowing MUC1 to interact with receptors that are normally restricted to the lateral and basal borders. In this regard, previous work has shown that MUC1 associates with members of the ErbB family of receptor tyrosine kinases in human breast cancer cells (13-15). Moreover, stimulation of cells with EGF or heregulin increased ErbB receptor-MUC1 complexes and tyrosine phosphorylation of the MUC1-CD (13-15). The present studies show that MUC1 also associates with FGFR3, another member of the receptor tyrosine kinase family. Importantly, activation of FGFR3 has been linked to the development of human malignancies; however, little is known about how FGFR3 contributes to transformation (38). FGFR3 is activated by its ligand FGF1 (19). As found with activation of ErbB receptors, stimulation of FGFR3 with FGF1 was associated with increased binding of FGFR3 and MUC1. In addition, stimulation of cells with FGF1 was associated with phosphorylation of MUC1 on Tyr^{46} in the cytoplasmic domain. As found with EGF, pretreatment of cells with PP2 blocked FGF1-induced phosphorylation of MUC1 on Tyr^{46}, indicating that this response to both growth factors is mediated by a c-Src-dependent mechanism. These findings indicate that, in addition to the ErbB receptors, MUC1 interacts with FGFR3 and that MUC1 may be of importance to intracellular signaling in cancers with FGFR3 mutations or overexpression.

FGF1 Induces Binding of MUC1 to β-Catenin

The MUC1-Tyr^{46} site is located just upstream to a SRM that binds to β-catenin (16). Previous work on cells stimulated with EGF showed that phosphorylation of MUC1 on Tyr^{46} induces

binding of MUC1 and β-catenin (13). In concert with these results, the present studies show that FGF1-induced phosphorylation of MUC1 on Tyr^{46} is also associated with increased binding of MUC1 and β-catenin. Moreover, expression of MUC1 with a Y46F mutation attenuated FGF1-induced formation of MUC1-β-catenin complexes. The MUC1 SRM binds directly to the β-catenin armadillo repeats and blocks glycogen synthase kinase 3β-mediated phosphorylation and degradation of β-catenin (46). MUC1-induced stabilization of β-catenin is also associated with increases in nuclear β-catenin and activation of Wnt target genes (46). We previously showed that MUC1 increases β-catenin levels in ZR-75-1 cells, but not in HCT116 cells, which express a mutant and thereby stable form of β-catenin (46). In concert with these results, FGF1-induced binding of MUC1 and β-catenin was associated with increased targeting of β-catenin to the nucleus of ZR-75-1 cells. By contrast, FGF1-induced binding of MUC1 and β-catenin had no effect on nuclear β-catenin levels in HCT116 cells. These findings indicate that MUC1 functions in integrating FGF1-induced signaling to β-catenin and thereby the Wnt pathway.

FGF1 Induces Binding of MUC1 to HSP90

Recent work has shown that MUC1 also forms intracellular complexes with HSP70 and HSP90 (39). The MUC1-CD binds directly to HSP70 (39). In addition, binding of MUC1 to HSP90 was found to be dependent on phosphorylation of MUC1 on Tyr^{46} (39). The present studies confirm the constitutive interaction between MUC1 and HSP70 and show that FGF1 stimulation has little if any effect on this interaction. We also found that FGF1-induced phosphorylation of MUC1 on Tyr^{46} stimulates binding of MUC1 to HSP90. Moreover, FGF1 increased the interaction between MUC1 and HSP90 by a mechanism that was attenuated by expressing MUC1 with the Y46F mutation. Geldanamycin, an inhibitor of the ATP-driven HSP90 chaperone cycle (51), also attenuated FGF1-induced binding of MUC1 to HSP90. Binding of HSP90 is associated with stabilization of certain client proteins (53). However, the finding that geldanamycin has no effect on MUC1 levels indicates that binding of this chaperone to MUC1 is not involved in the regulation of MUC1 stability. In this regard, the available evidence indicates that binding of MUC1 to complexes of HSP70 and HSP90 is responsible for delivery of MUC1 to the mitochondrial outer membrane (39).

Binding of MUC1 to β-Catenin and HSP70/HSP90 Is Mutually Exclusive

Our results indicate that FGF1-induced phosphorylation of MUC1 on Tyr^{46} increases binding of MUC1 to both β-catenin and HSP90. Whereas β-catenin binds to the SRM in the MUC1-CD (16, 46), the region responsible for the interaction with HSP90 has not been clear (39). Direct binding studies in the present work show that mutation of the SRM has no effect on binding of MUC1-CD to HSP70 but abrogates the interaction with HSP90. How HSP90 interacts with different client proteins is not precisely known; however, the available evidence indicates that HSP90 recognizes a surface structure rather than an amino acid sequence (54). Thus, our results suggest that the SRM may contribute to a surface structure on MUC1-CD that confers binding to HSP90. Consistent with involvement of the SRM, our studies further show that β-catenin competes with HSP90 for binding to MUC1-CD. In addition, β-catenin was effective, but to a lesser extent, in displacing HSP70 from MUC1-CD. These findings indicate that, following FGF1 stimulation and phosphorylation of MUC1 on Tyr^{46}, MUC1 can interact with either β-catenin or the HSP70/HSP90 complex (Fig. 7). The extent of MUC1 binding to β-catenin or HSP70/HSP90 complexes may be dictated by the relative intracellular levels of these proteins and/or other signals that are dependent on cell context. The findings also support a model in which intracellular trafficking of MUC1-C is in turn dictated by forming these mutually exclusive complexes (Fig. 7).

FGF1 Targets MUC1-C to the Nucleus

The MUC1-C, but not the MUC1-N, subunit trafficks to the nucleus (8-10, 15, 44-46, 55) and mitochondria (10, 39). The 20- to 25-kDa MUC1-C subunit includes the extracellular, transmembrane, and cytoplasmic domains (10). MUC1-C is also detectable as 17- and 15-kDa species (10); however, the precise structures of these forms are presently not known. The present studies indicate that FGF1 stimulation is associated with targeting of MUC1-C and β-catenin to the nucleus. The mechanism responsible for nuclear import of MUC1-C is not known, although MUC1-C associates with importin α and β, which function in transporting proteins to the nuclear pore.[1] β-Catenin is transported into the nucleus in the absence of importins and by a mechanism involving direct binding to the nuclear pore complex (56, 57). Thus, it is presently unclear whether MUC1-C and β-catenin are transported into the nucleus individually or as a complex. Nonetheless, MUC1-C and β-catenin colocalize within the nucleus (8, 44-46). In addition, MUC1-C coactivates β-catenin-mediated gene transcription (9, 46) by a mechanism involving MUC1-C occupancy with β-catenin on promoters of Wnt target genes.[1] These findings lend support to a model in which the FGF1-induced interaction between MUC1-C and β-catenin can transduce signals from the cell membrane to the nucleus that regulate gene expression (Fig. 7).

FGF1 Targets MUC1-C to Mitochondria

FGF1-induced targeting of MUC1-C to mitochondria was attenuated by geldanamycin, consistent with a mechanism in which HSP70/HSP90 complexes deliver client proteins to the mitochondrial outer membrane (52). By contrast, geldanamycin had no detectable effect on FGF1-induced targeting of MUC1-C to the nucleus (data not shown). These results collectively indicate that FGF1 activates two pathways in which MUC1-C is targeted to (*a*) the nucleus by a HSP90-independent mechanism and (*b*) mitochondria by a HSP90-dependent mechanism (Fig. 7). Delivery of MUC1-C to mitochondria is associated with integration of MUC1-C into the mitochondrial outer membrane (10, 39). The precise function of mitochondrial MUC1-C is not clear; however, localization of MUC1-C to the mitochondrial outer membrane is associated with attenuation of stress-induced (*a*) loss of mitochondrial transmembrane potential, (*b*) release

[1] Unpublished data.

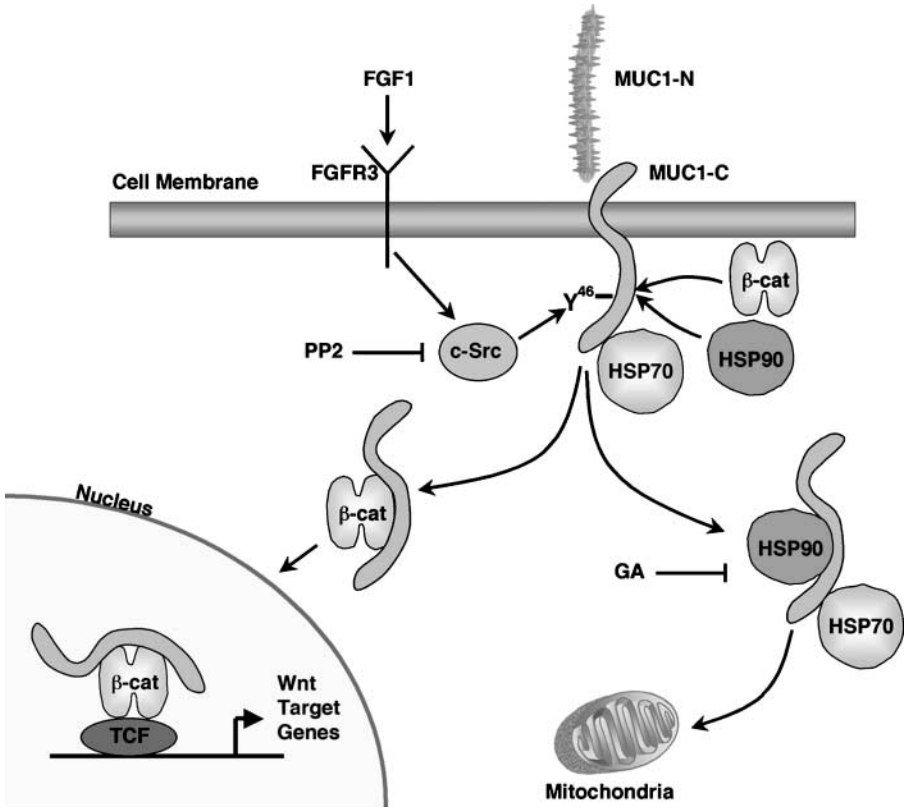

FIGURE 7. Model depicting FGF1-induced interactions between MUC1-C and β-catenin (*β-cat*) and MUC1-C and HSP90 that transduce signals from the cell membrane to the nucleus and mitochondria.

of mitochondrial apoptogenic factors, (*c*) activation of caspase-3, and (*d*) cell death (10, 58, 59). These findings thus support a model in which the FGF1-induced interaction between MUC1-C and HSP70/HSP90 complexes transduces signals from the cell membrane to mitochondria that attenuate activation of the intrinsic apoptotic pathway in the response to stress (Fig. 7).

Materials and Methods

Cell Culture

Human ZR-75-1, ZR-75-1/vector, and ZR-75-1/MUC1-siRNA breast cancer cells (10) were grown in RPMI 1640 containing 10% heat-inactivated fetal bovine serum, 100 units/mL penicillin, 100 μg/mL streptomycin, and 2 mmol/L L-glutamine. The ZR-75-1/MUC1siRNA cells were stably infected with a retrovirus expressing a siRNA that targets the 5′-GGTACCATCAATGTCCACG-3′ sequence encoding amino acids in the MUC1-C extracellular domain (10). The ZR-75-1/vector cells were infected with the empty retrovirus (10). HCT116/vector, HCT116/MUC1, and HCT116/MUC1(Y46F) cells (10) were cultured in DMEM/F12 with 10% heat-inactivated fetal bovine serum, 100 units/mL penicillin, and 100 μg/mL streptomycin. Human 293 embryonic kidney cells were grown in DMEM containing 10% heat-inactivated fetal bovine serum, antibiotics, and L-glutamine. Cells were cultured overnight in medium with 0.1% heat-inactivated fetal bovine serum and then stimulated with 30 ng/mL FGF1 (R&D Systems, Minneapolis, MN) in the presence of 7.5 μg/mL heparin (Sigma-Aldrich, St. Louis, MO), 20 ng/mL EGF (EMD Biosciences, La Jolla, CA), or 20 ng/mL heregulin (EMD Biosciences) at 37°C. Cells were also treated with 10 μmol/L PP2 (EMD Biosciences), 1 μmol/L geldanamycin (EMD Biosciences), or 17-AAG (EMD Biosciences).

Immunoprecipitation and Immunoblotting

Cell lysates prepared as described (10) were incubated with anti-FGFR3 (Sigma-Aldrich), anti-MUC1-N (monoclonal antibody DF3; ref. 1), anti-GFP (Clontech, Palo Alto, CA), anti-HSP70 (BD Biosciences, Palo Alto, CA), anti-HSP90 (BD Biosciences), or nonimmune IgG (Santa Cruz Biotechnology, Santa Cruz, CA) for 2 hours at 4°C. Immune complexes were subjected to immunoblotting with anti-MUC1-N, anti-FGFR3, anti-GFP, anti-MUC1-C (Ab5, NeoMarkers, Fremont, CA), anti-β-catenin (Zymed Laboratories, Carlsbad, CA), anti-HSP70, and anti-HSP90. Lysates not subjected to precipitation were immunoblotted with anti-phosphorylated MUC1-Tyr^{46} (Cell Signaling Technology, Danvers, MA), anti-MUC1-C, anti-β-actin (Sigma-Aldrich), anti-platelet-derived growth factor receptor (EMD Biosciences), anti-BAP31 (Abcam, Cambridge, MA), anti-Tom20 (BD Biosciences), anti-IκBα (Santa Cruz Biotechnology), anti-lamin B (EMD Biosciences), anti-HSP60 (Stressgen Bioreagents, Victoria, B.C., Canada), and anti-proliferating cell nuclear antigen (EMD Biosciences). Reactivity was detected with horseradish peroxidase–conjugated secondary antibodies and chemiluminescence (PerkinElmer Life Sciences, Wellesley, MA). Intensity of the signals was determined by densitometric scanning. Statistical significance was determined by Student's *t* test.

Cell Transfections

Sequences encoding MUC1-CD, MUC1-CD(1-45), or MUC1-CD(46-72) were amplified by PCR and cloned into

the pEGFP-C1 vector (Clontech). Transient transfections were done in the presence of LipofectAMINE (Invitrogen Life Technologies, Carlsbad, CA).

Subcellular Fractionation

Cytosolic and nuclear fractions were purified as described (60, 61). Mitochondria were prepared as described (10).

Binding Studies

Purified glutathione *S*-transferase (GST), GST-MUC1-CD, and GST-MUC1-CD(mSRM) in which the SRM SAGNGGSSLS was mutated to AAGNGGAAAA (39, 46) were bound to glutathione beads and incubated with recombinant human HSP70 or HSP90 (Stressgen Bioreagents) for 1 hour at 4°C. In certain experiments, the purified GST fusion proteins bound to glutathione beads were incubated with or without 50 ng c-Src (Upstate Biotechnology, Lake Placid, NY) in the presence of 200 μmol/L ATP for 30 minutes at 30°C. HSP90 was then added and the reaction was incubated for 1 hour at 4°C. For competition studies, HSP70 bound to GST-MUC1-CD or HSP90 bound to c-Src-phosphorylated GST-MUC1-CD was incubated with increasing amounts of β-catenin for 2 hours at 4°C. Precipitated proteins were subjected to immunoblot analysis.

Acknowledgments

We thank Dr. Q. Ge (Cell Signaling Technology) for the anti-phosphorylated MUC1-Tyr^{46} antibody and Kamal Chauhan for technical support.

References

1. Kufe D, Inghirami G, Abe M, et al. Differential reactivity of a novel monoclonal antibody (DF3) with human malignant versus benign breast tumors. Hybridoma 1984;3:223–32.

2. Ligtenberg MJ, Kruijshaar L, Buijs F, et al. Cell-associated episialin is a complex containing two proteins derived from a common precursor. J Biol Chem 1992;267:6171–7.

3. Levitin F, Stern O, Weiss M, et al. The MUC1 SEA module is a self-cleaving domain. J Biol Chem 2005;280:33374–6.

4. Macao B, Johansson DG, Hansson GC, Hard T. Autoproteolysis coupled to protein folding in the SEA domain of the membrane-bound MUC1 mucin. Nat Struct Mol Biol 2006;13:71–6.

5. Gendler S, Taylor-Papadimitriou J, Duhig T, Rothbard J, Burchell JA. A highly immunogenic region of a human polymorphic epithelial mucin expressed by carcinomas is made up of tandem repeats. J Biol Chem 1988;263:12820–3.

6. Siddiqui J, Abe M, Hayes D, et al. Isolation and sequencing of a cDNA coding for the human DF3 breast carcinoma-associated antigen. Proc Natl Acad Sci U S A 1988;85:2320–3.

7. Merlo G, Siddiqui J, Cropp C, et al. DF3 tumor-associated antigen gene is located in a region on chromosome 1q frequently altered in primary human breast cancer. Cancer Res 1989;49:6966–71.

8. Li Y, Liu D, Chen D, Kharbanda S, Kufe D. Human DF3/MUC1 carcinoma-associated protein functions as an oncogene. Oncogene 2003;22:6107–10.

9. Huang L, Ren J, Chen D, et al. MUC1 cytoplasmic domain coactivates Wnt target gene transcription and confers transformation. Cancer Biol Ther 2003;2:702–6.

10. Ren J, Agata N, Chen D, et al. Human MUC1 carcinoma-associated protein confers resistance to genotoxic anti-cancer agents. Cancer Cell 2004;5:163–75.

11. Wei X, Xu H, Kufe D. Human MUC1 oncoprotein regulates p53-responsive gene transcription in the genotoxic stress response. Cancer Cell 2005;7:167–78.

12. Schroeder JA, Adriance MC, Thompson MC, Camenisch TD, Gendler SJ. MUC1 alters β-catenin-dependent tumor formation and promotes cellular invasion. Oncogene 2003;22:1324–32.

13. Li Y, Ren J, Yu W-H, et al. The EGF receptor regulates interaction of the human DF3/MUC1 carcinoma antigen with c-Src and β-catenin. J Biol Chem 2001;276:35239–42.

14. Schroeder J, Thompson M, Gardner M, Gendler S. Transgenic MUC1 interacts with epidermal growth factor receptor and correlates with mitogen-activated protein kinase activation in the mouse mammary gland. J Biol Chem 2001;276:13057–64.

15. Li Y, Yu W-H, Ren J, et al. Heregulin targets γ-catenin to the nucleolus by a mechanism dependent on the DF3/MUC1 protein. Mol Cancer Res 2003;1:765–75.

16. Yamamoto M, Bharti A, Li Y, Kufe D. Interaction of the DF3/MUC1 breast carcinoma-associated antigen and β-catenin in cell adhesion. J Biol Chem 1997;272:12492–4.

17. Li Y, Bharti A, Chen D, Gong J, Kufe D. Interaction of glycogen synthase kinase 3β with the DF3/MUC1 carcinoma-associated antigen and β-catenin. Mol Cell Biol 1998;18:7216–24.

18. Li Y, Kuwahara H, Ren J, Wen G, Kufe D. The c-Src tyrosine kinase regulates signaling of the human DF3/MUC1 carcinoma-associated antigen with GSK3β and β-catenin. J Biol Chem 2001;276:6061–4.

19. Johnson DE, Williams LT. Structural and functional diversity in the FGF receptor multigene family. Adv Cancer Res 1993;60:1–41.

20. Webster MK, Donoghue DJ. FGFR activation in skeletal disorders: too much of a good thing. Trends Genet 1997;13:178–82.

21. Hattori Y, Odagiri H, Katoh O, et al. K-sam-related gene, N-sam, encodes fibroblast growth factor receptor and is expressed in T-lymphocytic tumors. Cancer Res 1992;52:3367–71.

22. Popovici C, Adelaide J, Ollendorff V, et al. Fibroblast growth factor receptor 1 is fused to FIM in stem-cell myeloproliferative disorder with t(8;13). Proc Natl Acad Sci U S A 1998;95:5712–7.

23. Reiter A, Sohal J, Kulkarni S, et al. Consistent fusion of ZNF198 to the fibroblast growth factor receptor-1 in the t(8;13)(p11;q12) myeloproliferative syndrome. Blood 1998;92:1735–42.

24. Tavormina PL, Bellus GA, Webster MK, et al. A novel skeletal dysplasia with developmental delay and acanthosis nigricans is caused by a Lys650Met mutation in the fibroblast growth factor receptor 3 gene. Am J Hum Genet 1999;64:722–31.

25. Sibley K, Stern P, Knowles MA. Frequency of fibroblast growth factor receptor 3 mutations in sporadic tumours. Oncogene 2001;20:4416–8.

26. Cappellen D, De Oliveira C, Ricol D, et al. Frequent activating mutations of FGFR3 in human bladder and cervix carcinomas. Nat Genet 1999;23:18–20.

27. Chesi M, Nardini E, Brents LA, et al. Frequent translocation t(4;14)(p16.3;q32.3) in multiple myeloma is associated with increased expression and activating mutations of fibroblast growth factor receptor 3. Nat Genet 1997;16:260–4.

28. Richelda R, Ronchetti D, Baldini L, et al. A novel chromosomal translocation t(4; 14)(p16.3; q32) in multiple myeloma involves the fibroblast growth-factor receptor 3 gene. Blood 1997;90:4062–70.

29. Chesi M, Nardini E, Lim RS, et al. The t(4;14) translocation in myeloma dysregulates both FGFR3 and a novel gene, MMSET, resulting in IgH/MMSET hybrid transcripts. Blood 1998;92:3025–34.

30. Ishikawa H, Tsuyama N, Liu S, et al. Accelerated proliferation of myeloma cells by interleukin-6 cooperating with fibroblast growth factor receptor 3-mediated signals. Oncogene 2005;24:6328–32.

31. Malgeri U, Baldini L, Perfetti V, et al. Detection of t(4;14)(p16.3;q32) chromosomal translocation in multiple myeloma by reverse transcription-polymerase chain reaction analysis of IGH-MMSET fusion transcripts. Cancer Res 2000;60:4058–61.

32. Zhu L, Somlo G, Zhou B, et al. Fibroblast growth factor receptor 3 inhibition by short hairpin RNAs leads to apoptosis in multiple myeloma. Mol Cancer Ther 2005;4:787–98.

33. Gomez-Roman JJ, Saenz P, Molina M, et al. Fibroblast growth factor receptor 3 is overexpressed in urinary tract carcinomas and modulates the neoplastic cell growth. Clin Cancer Res 2005;11:459–65.

34. Su Y, Han J, Xu S, Cobb M, Skolnik E. NIK is a new Ste20-related kinase that binds NCK and MEKK1 and activates the SAPK/JNK cascade via a conserved regulatory domain. EMBO J 1997;16:1279–90.

35. Sahni M, Ambrosetti DC, Mansukhani A, et al. FGF signaling inhibits chondrocyte proliferation and regulates bone development through the STAT-1 pathway. Genes Dev 1999;13:1361–6.

36. Hart KC, Robertson SC, Donoghue DJ. Identification of tyrosine residues in constitutively activated fibroblast growth factor receptor 3 involved in mitogenesis, Stat activation, and phosphatidylinositol 3-kinase activation. Mol Biol Cell 2001;12:931–42.

37. Kong M, Wang CS, Donoghue DJ. Interaction of fibroblast growth factor receptor 3 and the adapter protein SH2-B. A role in STAT5 activation. J Biol Chem 2002;277:15962–70.

38. L'Hote CG, Knowles MA. Cell responses to FGFR3 signalling: growth, differentiation, and apoptosis. Exp Cell Res 2005;304:417–31.

39. Ren J, Bharti A, Raina D, et al. MUC1 oncoprotein is targeted to mitochondria by heregulin-induced activation of c-Src and the molecular chaperone HSP90. Oncogene 2006;25:20–31.

40. Perey L, Hayes DF, Maimonis P, et al. Tumor selective reactivity of a monoclonal antibody prepared against a recombinant peptide derived from the DF3 human breast carcinoma-associated antigen. Cancer Res 1992;52:2563–3568.

41. Rahn JJ, Dabbagh L, Pasdar M, Hugh JC. The importance of MUC1 cellular localization in patients with breast carcinoma: an immunohistologic study of 71 patients and review of the literature. Cancer 2001;91:1973–82.

42. Croce MV, Isla-Larrain MT, Rua CE, et al. Patterns of MUC1 tissue expression defined by an anti-MUC1 cytoplasmic tail monoclonal antibody in breast cancer. J Histochem Cytochem 2003;51:781–8.

43. Ng FW, Nguyen M, Kwan T, et al. p28 Bap31, a Bcl-2/Bcl-XL- and procaspase-8-associated protein in the endoplasmic reticulum. J Cell Biol 1997; 139:327–38.

44. Li Y, Chen W, Ren J, et al. DF3/MUC1 signaling in multiple myeloma cells is regulated by interleukin-7. Cancer Biol Ther 2003;2:187–93.

45. Wen Y, Caffrey T, Wheelock M, Johnson K, Hollingsworth M. Nuclear association of the cytoplasmic tail of MUC1 and β-catenin. J Biol Chem 2003; 278:38029–39.

46. Huang L, Chen D, Liu D, et al. MUC1 oncoprotein blocks GSK3β-mediated phosphorylation and degradation of β-catenin. Cancer Res 2005;65:10413–22.

47. Morin PJ, Sparks AB, Korinek V, et al. Activation of β-catenin-Tcf signaling in colon cancer by mutations in β-catenin or APC. Science 1997;275:1787–90.

48. Morin PJ. β-Catenin signaling and cancer. BioEssays 1999;21:1021–30.

49. Polakis P. Wnt signaling and cancer. Genes Dev 2000;14:1837–51.

50. Liu C, Li Y, Semenov M, et al. Control of β-catenin phosphorylation/ degradation by a dual-kinase mechanism. Cell 2002;108:837–47.

51. Whitesell L, Mimnaugh EG, De Costa B, Myers CE, Neckers LM. Inhibition of heat shock protein HSP90-pp60v-src heteroprotein complex formation by benzoquinone ansamycins: essential role for stress proteins in oncogenic transformation. Proc Natl Acad Sci U S A 1994;91:8324–8.

52. Young JC, Hoogenraad NJ, Hartl FU. Molecular chaperones Hsp90 and Hsp70 deliver preproteins to the mitochondrial import receptor Tom70. Cell 2003; 112:41–50.

53. Isaacs JS, Xu W, Neckers L. Heat shock protein 90 as a molecular target for cancer therapeutics. Cancer Cell 2003;3:213–7.

54. Citri A, Harari D, Shohat G, et al. Hsp90 recognizes a common surface on client kinases. J Biol Chem 2006;281:14361–9.

55. Baldus SE, Monig SP, Huxel S, et al. MUC1 and nuclear β-catenin are coexpressed at the invasion front of colorectal carcinomas and are both correlated with tumor prognosis. Clin Cancer Res 2004;10:2790–6.

56. Fagotto F, Gluck U, Gumbiner BM. Nuclear localization signal-independent and importin/karyopherin-independent nuclear import of β-catenin. Curr Biol 1998;8:181–90.

57. Henderson BR, Fagotto F. The ins and outs of APC and β-catenin nuclear transport. EMBO Rep 2002;3:834–9.

58. Yin L, Kufe D. Human MUC1 carcinoma antigen regulates intracellular oxidant levels and the apoptotic response to oxidative stress. J Biol Chem 2003; 278:35458–64.

59. Yin L, Huang L, Kufe D. MUC1 oncoprotein activates the FOXO3a transcription factor in a survival response to oxidative stress. J Biol Chem 2004; 279:45721–7.

60. Kharbanda S, Saleem A, Yuan Z-M, et al. Nuclear signaling induced by ionizing radiation involves colocalization of the activated p56/p53^{lyn} tyrosine kinase with p34^{cdc2}. Cancer Res 1996;56:3617–21.

61. Datta R, Oki E, Endo K, et al. XIAP regulates DNA damage-induced apoptosis downstream of caspase-9 cleavage. J Biol Chem 2000;275:31733–8.